Article

Tethered Dinuclear Europium(III) Macrocyclic Catalysts for the Cleavage of RNA

Kido Nwe, Christopher M. Andolina, and Janet R. Morrow

J. Am. Chem. Soc., **2008**, 130 (44), 14861-14871 • DOI: 10.1021/ja8037799 • Publication Date (Web): 10 October 2008

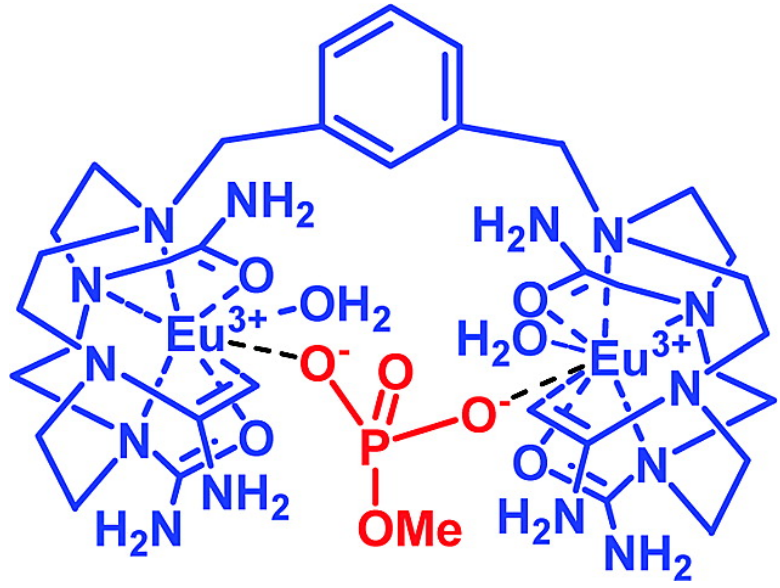

More About This Article

Additional resources and features associated with this article are available within the HTML version:

- Supporting Information
- Access to high resolution figures
- Links to articles and content related to this article
- Copyright permission to reproduce figures and/or text from this article

View the Full Text HTML

J|A|C|S
ARTICLES

Published on Web 10/10/2008

Tethered Dinuclear Europium(III) Macrocyclic Catalysts for the Cleavage of RNA

Kido Nwe, Christopher M. Andolina, and Janet R. Morrow*

Department of Chemistry, University at Buffalo, State University of New York, Amherst, New York 14260-3000

Received May 20, 2008; E-mail: jmorrow@buffalo.edu

Abstract: Dinuclear europium(III) complexes of the macrocycles 1,3-bis[1-(4,7,10-tris(carbamoylmethyl)-1,4,7,10-tetraazacyclododecane]-*m*-xylene (**1**), 1,4-bis[1-(4,7,10-tris(carbamoylmethyl)-1,4,7,10-tetraazacyclododecane]-*p*-xylene (**2**), and mononuclear europium(III) complexes of macrocycles 1-methyl-,4,7,10-tris(carbamoylmethyl)-1,4,7,10-tetraazacyclododecane (**3**), 1-[3′-(*N*,*N*-diethylaminomethyl)benzyl]-4,7,10-tris(carbamoylmethyl)-1,4,7,10-tetraazacyclododecane (**4**), and 1,4,7-tris(carbamoylmethyl)-1,4,7,10-tetraazacyclododecane (**5**) were prepared. Studies using direct excitation ($^7F_0 \rightarrow {}^5D_0$) europium(III) luminescence spectroscopy show that each Eu(III) center in the mononuclear and dinuclear complexes has two water ligands at pH 7.0, $I = 0.10$ M ($NaNO_3$) and that there are no water ligand ionizations over the pH range of 7−9. All complexes promote cleavage of the RNA analogue 2-hydroxypropyl-4-nitrophenyl phosphate (**HpPNP**) at 25 °C ($I = 0.10$ M ($NaNO_3$), 20 mM buffer). Second-order rate constants for the cleavage of **HpPNP** by the catalysts increase linearly with pH in the pH range of 7−9. The second-order rate constant for **HpPNP** cleavage by the dinuclear Eu(III) complex (Eu_2(**1**)) at pH 7 is 200 and 23-fold higher than that of Eu(**5**) and Eu(**3**), respectively, but only 7-fold higher than the mononuclear complex with an aryl pendent group, Eu(**4**). This shows that the macrocycle substituent modulates the efficiency of the Eu(III) catalysts. Eu_2(**1**) promotes cleavage of a dinucleoside, uridylyl-3′,5′-uridine (**UpU**) with a second-order rate constant at pH 7.6 (0.021 M^{-1} s^{-1}) that is 46-fold higher than that of the mononuclear Eu(**5**) complex. Methyl phosphate binding to the Eu(III) complexes is energetically most favorable for the best catalysts, and this supports an important role for the catalyst in stabilization of the developing negative charge on the phosphorane transition state. Despite the formation of a bridging phosphate ester between the two Eu(III) centers in Eu_2(**1**) as shown by luminescence spectroscopy, the two metal ion centers are only weakly cooperative in cleavage of RNA and RNA analogues.

Introduction

It has been long suspected that the unique coordination properties of lanthanide ions including their high charge, large ionic radii, variable coordination geometry, and oxophilicity give rise to their phenomenal efficiency as catalysts for the cleavage of RNA.[1−12] Efforts to unravel the mechanism of lanthanide ions in catalysis, however, have been hampered by the complexity of lanthanide ion solution chemistry.[1,10,13] We have reported the use of direct excitation lanthanide luminescence spectroscopy to characterize the solution speciation of Eu(III) catalysts[3,14−16] and to define the differences in coordination properties between lanthanide ion catalysts and the better understood Zn(II) catalysts.[17−21] Eu(III) excitation luminescence spectroscopy is a powerful technique for the identification of aqua and hydroxide Eu(III) complexes,[14,22] their dimerization,[23−25] and their binding constants to ligands and substrates.[26,27]

(1) Aguilar-Perez, F.; Gomez-Tagle, P.; Collado-Fregoso, E.; Yatsimirsky, A. K. *Inorg. Chem.* **2006**, *45*, 9502–9517.
(2) Hall, J.; Husken, D.; Pieles, U.; Moser, H. E.; Haner, R. *Chem. Biol.* **1994**, *1*, 185–190.
(3) Amin, S.; Voss, D. A.; Horrocks, W. D.; Morrow, J. R. *Inorg. Chem.* **1996**, *35*, 7466–7467.
(4) Fanning, A.-M.; Plush, S. E.; Gunnlaugsson, T. *Chem. Commun.* **2006**, 3791–3793.
(5) Hurst, P.; Takasaki, B. K.; Chin, J. *J. Am. Chem. Soc.* **1996**, *118*, 9982–9983.
(6) Husken, D.; Goodall, G.; Blommers, M. J. J.; Jahnke, W.; Hall, J.; Haner, R.; Moser, H. E. *Biochemistry* **1996**, *35*, 16591–16600.
(7) Magda, D.; Wright, M.; Crofts, S.; Lin, A.; Sessler, J. L. *J. Am. Chem. Soc.* **1997**, *119*, 6947–6948.
(8) Magda, D.; Miller, R. A.; Sessler, J. L.; Iverson, B. L. *J. Am. Chem. Soc.* **1994**, *116*, 7439–7440.
(9) Amin, S.; Morrow, J. R.; Lake, C. H.; Churchill, M. R. *Angew. Chem., Int. Ed. Engl.* **1994**, *33*, 773–775.
(10) Jurek, P. E.; Jurek, A. M.; Martell, A. E. *Inorg. Chem.* **2000**, *39*, 1016–1020.
(11) Komiyama, M.; Takeda, N.; Shigekawa, H. *Chem. Commun.* **1999**, 1443–1451.
(12) Yashiro, M.; Ishikubo, A.; Komiyama, M. *J. Biochem. (Tokyo)* **1996**, *120*, 1067–1069.
(13) Chang, C. A.; Wu, B. H.; Kuan, B. Y. *Inorg. Chem.* **2005**, *44*, 6646–6654.
(14) Amin, S.; Voss, D. A.; Horrocks, W. D.; Lake, C. H.; Churchill, M. R.; Morrow, J. R. *Inorg. Chem.* **1995**, *34*, 3294–3300.
(15) Voss, D. A.; Farquhar, E. R.; Horrocks, W. D.; Morrow, J. R. *Inorg. Chim. Acta* **2004**, *357*, 859–863.
(16) Nwe, K.; Richard, J. P.; Morrow, J. R. *Dalton Trans.* **2007**, 5171–5178.
(17) Feng, G.; Natale, D.; Prabaharan, R.; Mareque-Rivas, J. C.; Williams, N. H. *Angew. Chem., Int. Ed.* **2006**, *45*, 7056–7059.
(18) O'Donoghue, A.; Pyun, S. Y.; Yang, M. Y.; Morrow, J. R.; Richard, J. P. *J. Am. Chem. Soc.* **2006**, *128*, 1615–1621.
(19) Yang, M. Y.; Iranzo, O.; Richard, J. P.; Morrow, J. R. *J. Am. Chem. Soc.* **2005**, *127*, 1064–1065.
(20) Iranzo, O.; Kovalevsky, A. Y.; Morrow, J. R.; Richard, J. P. *J. Am. Chem. Soc.* **2003**, *125*, 1988–1993.
(21) Feng, G.; Mareque-Rivas, J. C.; Martin de Rosales, R.; Williams, N. H. *J. Am. Chem. Soc.* **2005**, *127*, 13470–13471.
(22) Horrocks, W. D.; Sudnick, D. R. *J. Am. Chem. Soc.* **1979**, *101*, 334–340.

Even more challenging than the study of mononuclear Eu(III) complexes is the design and characterization of effective dinuclear lanthanide ion catalysts. Our past work with self-assembled dinuclear lanthanide catalysts containing a bridging hydroxide ligand showed that there was little cooperativity between metal ion centers for the cleavage of phosphate diesters.[28] Other reported self-assembled multinuclear lanthanide complexes contain weakly bound ligands and bridging hydroxides that lead to cooperative behavior of the two metal ion centers toward phosphate diester cleavage.[1,5] The fragile nature of these highly reactive complexes makes it difficult to define the solution speciation of these systems and to probe the mechanism of catalytic cleavage.

Here we present studies of two dinuclear Eu(III) macrocyclic complexes that have two coordination sites on each Eu(III) ion center for catalysis. Cleavage of an RNA model, 2-hydroxypropyl-4-nitrophenyl phosphate (**HpPNP**), and a dinucleoside, uridylyl-3′,5′-uridine (**UpU**), by these dinuclear catalysts is compared to their mononuclear analogues to gauge the extent of lanthanide ion cooperativity in the dinuclear catalysts. These comparisons are further illuminated by characterization of solution speciation and Eu(III) complex binding to carbonate and to phosphate esters that are substrate and transition state analogues. Despite the lack of Ln(III) ion cooperativity in catalysis, the tethered dinuclear lanthanide ion complexes presented here are among the most active metal ion macrocyclic catalysts for dinucleoside and RNA analogue cleavage in water at 25 °C that have been reported to date. Direct excitation luminescence spectroscopy provides a unique opportunity to fully characterize the coordination properties of these active catalysts including the surprising absence of hydroxide ligands and the formation of bridging phosphate ester complexes.

Experimental Section

Cyclen (1,4,7,10-tetraazacyclododecane) was purchased from Strem chemicals. Acetonitrile and methanol were dried over calcium hydride. **HpPNP**,[29] 1,4,7-tris(carbamoylmethyl)-1,4,7,10-tetraazacyclododecane (**5**), and Eu(**5**) were prepared as reported earlier.[16] Uridylyl(3′,5′)uridine (**UpU**, NH_4^+ salt), uridine (2′,3′)-cyclic monophosphate (2′,3′-cUMP), uridine 3′-monophosphate (3′-UMP), uridine 2′-monophosphate (2′-UMP), and uridine were reagent grade from Sigma-Aldrich. Milli-Q purified water was boiled and bubbled with nitrogen gas for 1 h prior to use in kinetic experiments or in luminescence measurements to minimize carbonate concentrations. An Orion research digital ionalyzer, model 510, equipped with a temperature compensation probe was used for all pH measurements. All ^{1}H and ^{13}C NMR were recorded on either a Gemini-300, Inova-400, or Inova-500 spectrometer.

Syntheses. 1,3-Bis[1-(4,7,10-tris(carbamoylmethyl)-1,4,7,10-tetraazacyclododecane]-*m*-xylene (1). To 0.500 g (1.25 mmol) of compound **6** (1,3-bis-(1,4,7,10-tetraazacyclododecane))[30] was added 1.04 g (7.54 mmol) of K_2CO_3 and 1.04 g (7.60 mmol) of bromoacetamide in 30 mL of absolute ethanol. The solution was stirred at 80 °C overnight under nitrogen. Solid K_2CO_3 was filtered off, and the solvent was removed under vacuum. The residue was dissolved in a minimum amount of methanol, and chloroform was added. The supernatant was filtered off,and the resulting white precipitate was dried under vacuum. Yield: 90%. ESI *m*/*z*: 789 (M + 1), 827 (M + K), 811 (M + Na). ^{1}H NMR (500 MHz, D_2O): δ = 2.55−3.25 (44 H, m, ring CH_2, NCH_2CONH$_2$), 4.2 (4H, s, ArCH_2N), 7.54 (2H, m, Ph), 7.45 (2H, m, Ph). ^{13}C NMR (300 MHz, D_2O): δ = 49.50, 50.85, 51.21, 51.76, 55.78, 56.3 (ring CH_2 and NCH_2CONH$_2$), 68.9 (ArCH_2N), 130.8, 132.1, 134.0 (Ph), 175.2, 176.4 (C═O).

1,4-Bis[1-(4,7,10-tris(carbamoylmethyl)-1,4,7,10-tetraazacyclododecane]-*p*-xylene (2). A procedure similar to that described for **1** was used to produce a white solid in 90% yield from compound **7** (1,4-bis-(1,4,7,10-tetraazacyclododecane)).[30] ESI *m*/*z*: 789 (M + 1), 827 (M + K). ^{1}H NMR (500 MHz, D_2O): δ = 2.45−3.15 (40 H, m, ring CH_2, NCH_2CONH$_2$), 3.22 (s, 4H, NCH_2CONH$_2$), 3.85 (s, 4H, NCH_2Ar), 7.30 (s, 4H, Ph). ^{13}C NMR (300 MHz, D_2O): δ = 50.5, 51.3, 51.5, 52.3, 56.3, 57.0, 58.3 (ring CH_2 and NCH_2CONH$_2$ and ArCH_2N), 130.8, 163.8 (Ph), 176.2, 177.2 (C═O).

1-[3′-(*N*,*N*-Diethylaminomethyl)benzyl]-4,7,10-tris(ter-butoxycarbonyl)-1,4,7,10-tetraazacyclododecane (9). An acetonitrile solution containing **8** (1-[3′-(bromomethyl)benzyl]-4,7,10-tris(ter-butoxycarbonyl)-1,4,7,10-tetraazacyclododecane)[31] (1.00 g, 1.53 mmol) and diethylamine (200 μL, 2.08 mmol) was stirred at room temperature for 6 h. The solvent was removed under vacuum. The resulting crude product was washed with hexanes and dried twice to obtain a pale yellow solid which was used without further purification. Yield 90%. ESI *m*/*z*: 648 (M + 1). ^{1}H NMR (500 MHz, $CDCl_3$): δ = 1.20 (6H, t, CH_2CH_3), 1.42 (18 H, m, CH_3), 1.48 (9H, m, CH_3), 2.65 (8H, m, ring CH_2, CH_2CH_3), 3.2−3.81 (28H, m, ring CH_2, ArCH_2N, ArCH_2N(CH_2CH_3)$_2$), 7.22−7.4 (4H, m, Ph). ^{13}C NMR (300 MHz, $CDCl_3$): δ = 11.0 (CH_2CH_3) 29.0, 29.4 (CH_3; *t*-but), 47.2 (CH_2CH_3), 48.4, 50.1, 55.1, 56.2, 57.5, 65.7, 72.8 (ring CH_2 and ArCH_2N(CH_2CH_3)$_2$ and ArCH_2N), 80.1 (C(CH_3)$_3$), 128.1, 129.3, 129.8, 130.4, 132.0, 137.5 (Ph), 156.0, 156.4, 156.8 (C═O).

1-[3′-(*N*,*N*-Diethylaminomethyl)benzyl]-1,4,7,10-tetraazacyclododecane (10). Compound **9** (1.00 g, 1.55 mmol) was dissolved in 20 mL of ethanol, and 7 mL of concentrated hydrochloric acid was slowly added. The solution was stirred at room temperature for 8 h during which time a precipitate formed. The precipitate was filtered, washed with ethanol, and dried. The dried hydrochloride salt was then dissolved in a minimum amount of water, and the pH was adjusted to 12.5. The solution was extracted with dichloromethane, and the organic layer was dried over anhydrous sodium sulfate. The solvent was removed to yield a pale yellow solid. (yield, 85%). ESI *m*/*z*: 348 (M + 1). ^{1}H NMR (500 MHz, D_2O): δ = 1.2 (6H, t, CH_2CH_3), 2.8−3.7 (24H, m, ring CH_2, CH_2CH_3), 3.9 (2H, s, ArCH_2N), 4.2 (2H, s, ArCH_2N(CH_2CH_3)$_2$), 7.2−7.6 (4H, m, Ph). ^{13}C NMR (300 MHz, D_2O): δ = 8.10 (NCH$_2$$CH_3$), 41.9 (N$CH_2CH_3$), 42.2, 43.8, 44.3, 46.9 (ring CH_2), 55.7 56.5 (ArCH_2N and ArCH_2N(CH_2CH_3)$_2$), 129.8, 130.1, 130.9, 131.7, 132.7, 135.3 (Ph).

1-[3′-(*N*,*N*-Diethylaminomethyl)benzyl]-4,7,10-tris(carbamoylmethyl)-1,4,7,10-tetraazacyclododecane (4). Bromoacetamide (0.60 g, 4.32 mmol), compound **10** (0.50 g, 1.44 mmol) and K_2CO_3

(23) Brittain, H. G.; Mantha, S.; Tweedle, M. F. *J. Less-Common Met.* **1986**, *126*, 339–342.
(24) Hernandez, G.; Brittain, H. G.; Tweedle, M. F.; Bryant, R. G. *Inorg. Chem.* **1990**, *29*, 985–988.
(25) Zhang, X.; Chang, C. A.; Brittain, H. G.; Garrison, J. M.; Telser, J.; Tweedle, M. F. *Inorg. Chem.* **1992**, *31*, 5597–5600.
(26) Epstein, D. M.; Chappell, L. L.; Khalili, H.; Supkowski, R. M.; Horrocks, W. D., Jr.; Morrow, J. R. *Inorg. Chem.* **2000**, *39*, 2130–2134.
(27) Supkowski, R. M.; Horrocks, W. D. *Inorg. Chem.* **1999**, *38*, 5616–5619.
(28) Farquhar, E. R.; Richard, J. P.; Morrow, J. R. *Inorg. Chem.* **2007**, *46*, 7169–7177.
(29) Brown, D. M.; Usher, D. A. *J. Chem. Soc.* **1965**, 6558–6564.
(30) Le Baccon, M.; Chuburu, F.; Toupet, L.; Handel, H.; Soibinet, M.; Dechamps-Olivier, I.; Barbier, J.-P.; Aplincourt, M. *New J. Chem.* **2001**, *25*, 1168–1174.
(31) Xia, C.-Q.; Jiang, N.; Zhang, J.; Chen, S.-Y.; Lin, H.-H.; Tan, X.-Y.; Yue, Y.; Yu, X.-Q. *Bioorg. Med. Chem.* **2006**, *14*, 5756–5764.

(0.60 g, 4.38 mmol) were added to absolute ethanol and the solution was heated to reflux for 4 h. The solution was filtered to remove inorganic salts, the supernatant was dried and the solvent was removed under vacuum. The resulting solid residue was washed with ethyl acetate and dried under high vacuum to obtain **4** as white solid (yield, 80%). ESI *m/z*: 541 (M + Na). ^{1}H NMR (500 MHz, CD_3OD): δ = 1.1 (6H, t, CH_2CH_3), 2.2−2.8 (16H, m, ring CH_2, $N(CH_2CH_3)_2$), 3.15 (4H, m, ring CH_2), 3.41 (2H, s, $ArCH_2N$), 3.46 (2H, s, $ArCH_2N(CH_2CH_3)_2$), 3.98, 4.08 (6H, s, NCH_2CONH_2), 7.22−7.4 (4H, m, Ph). ^{13}C NMR (300 MHz, CD_3OD): δ = 11.8 (CH_2CH_3), 47.5 (CH_2CH_3), 51.5, 52.5, 56.8, 58.5 (ring CH_2), 62.4, 68.6, 70.4 ($ArCH_2N(CH_2CH_3)_2$ and $ArCH_2N$ and NCH_2CONH_2), 129.6, 130.2, 130.6, 133.1, 137.6, 139.0 (Ph), 178.2 (C═O).

1-Methyl-,4,7,10-tris(carbamoylmethyl)-1,4,7,10-tetraazacyclododecane (3). Compound **5**[16] (0.140 g, 0.410 mmol), K_2CO_3 (0.410 g, 2.97 mmol), and 31 μL of CH_3I solution (99.8%) were added to absolute ethanol and heated to 75 °C overnight. The solid K_2CO_3 base was filtered, and the solvent was removed. The resulting solid residue was washed with ethyl acetate and dried to obtain a white solid (yield 90%). ESI *m/z*: 358 (M + 1). ^{1}H NMR (400 MHz, D_2O): δ = 2.58 (3H, s, CH_3), 2.50−2.81 (16H, m, ring CH_2), 3.02, 3.12 (2H, s, NCH_2CONH_2). ^{13}C NMR (300 MHz, D_2O): δ = 45.7(CH_3), 49.7, 52.0, 53.3, 59.5 56.4, 57.2 (ring CH_2 and NCH_2CONH_2), 176.9, 177.4 (C═O).

Eu(III) Complexes. Eu(III) complexes were prepared by refluxing $Eu(CF_3SO_3)_3$ and the macrocyclic ligands in dry methanol for 8 h. In a typical preparation, 0.200 g (0.254 mmol) of ligand **1** or **2** and 0.312 g (0.521 mmol) of $Eu(CF_3SO_3)_3$ were refluxed in 20 mL of dry methanol for 8 h. The same procedure was followed for the monomers except only 1.05 equiv of metal salt was utilized. For the complexes with ligand **1**, **2**, and **4**, the solvent was reduced to 1 mL and chloroform was slowly added until a precipitate formed at the bottom of the flask. The supernatant was decanted, and the solid was dried under vacuum to give a white solid. For the Eu(III) complex of ligand **3**, the solvent was reduced to 1 mL and chloroform was added until an oil formed. The oil was separated and dried under vacuum to give a solid. Eu_2(**1**): Yield 90%. Anal. Calcd for $C_{42}H_{64}N_{14}O_{24}F_{18}S_6Eu_2\cdot(CHCl_3)$: C 24.48, H 3.08, N 9.30. Found C 24.33, H 2.96, N 9.15. Eu_2(**2**): Yield 90%. Anal. Calcd for $C_{42}H_{64}N_{14}O_{24}F_{18}S_6Eu_2\cdot(3CHCl_3)$: C 23.74, H 2.99, N 8.81. Found C 23.72, H 2.80, N 8.65. Eu(**3**): Yield 90%. ESI *m/e*: 806, 808 ([Eu(**3**)]$(CF_3SO_3)_3$ − $CF_3SO_3^-$). Anal. Calcd for $C_{18}H_{31}N_7O_{12}F_9S_3Eu_1\cdot(3CHCl_3)(H_2O)$: C 19.80, H 2.91, N 8.08. Found C 19.87, H 2.91, N 7.96. Eu(**4**): Yield 90%. ESI *m/z*: 967, 969 ([Eu(**4**)]$(CF_3SO_3)_3$ − $CF_3SO_3^-$). Anal. Calcd for $C_{29}H_{46}N_8O_{12}F_9S_3Eu_1\cdot(2CHCl_3)(2H_2O)$: C 26.74, H 3.76, N 8.05. Found C 26.85, H 3.86, N 7.88.

Kinetic Measurements. A Beckman Coulter DU 640 UV−vis spectrophotometer with thermostatted cell compartment was utilized for kinetic measurements. Cleavage of **HpPNP** at 25.0 °C was followed by monitoring the increase in absorbance at 400 nm due to the formation of 4-nitrophenoxide anion. The following concentrations were used for the catalysts: Eu_2(**1**), Eu_2(**2**), and Eu(**3**) (0.20−1.0 mM), Eu(**4**) (0.10−0.50 mM), Eu(**5**) (0.20−2.0 mM). The pseudo-first-order rate constants k_{obsd} (s^{-1}) for these reactions were determined as the slopes of semilogarithmic plots of reaction progress ($A_\infty - A_t$) against time, where A_t is the observed absorbance at 400 nm and A_∞ is the final absorbance at the end of the reaction. For all reactions, the values of k_{obsd} were found to be reproducible to ±5%. Solutions contained 0.0200 M of the following buffers: MES (6.2−7.2), Hepes (6.8−7.7), EPPS (8.0−8.8), and CHES (8.8−10) with 0.10 M ($NaNO_3$) to maintain ionic strength. Cleavage of **HpPNP** (1.0 mM) in the presence of the Eu(III) catalysts at pH 8.0 gave rise to a single peak in the ^{31}P NMR spectrum at 18.6 ppm for the cyclic phosphate ester.

For inhibition studies, the same procedure was followed to prepare the samples and the concentration of the inhibitor was varied accordingly. The solution contained 0.10−0.50 mM Eu_2(**1**) or 0.10 mM Eu(**3**), 0−5.0 mM methyl phosphate (**MP**) or 0−20 mM diethyl phosphate (**DEP**), 20 mM buffer, and 0.10 M $NaNO_3$. The data were fit to eq 1.[32] Here k_{obsd} and k_0 are observed rate constants of cleavage in the presence and absence of phosphate ester, respectively, $[A]_t$ is the total concentration of phosphate ester, $[Eu]_t$ is total concentration of the catalyst, and K_i is the inhibition constant.

$$\frac{k_{obsd}}{k_0} = \left(\frac{[Eu]_t - [A]_t - K_i + \sqrt{[Eu]_t^2 + [A]_t^2 + K_i^2 - 2[Eu]_t[A]_t + 2[Eu]_tK_i + 2K_i[A]_t}}{2[Eu]_t}\right) \quad (1)$$

Cleavage of UpU. The cleavage of **UpU** was monitored by separating the reactant and the products over a C18 Varian microsorb-mv column (250 mm × 4.6 mm; 5 μm) using a Beckman System Gold high-performance liquid chromatograph (HPLC) equipped with 168 UV−vis detector with peak detection at 260 nm. The elution was isocratic with a pH 4.3 buffer (20 mM ammonium acetate) with the flow rate of 1 mL/min from t = 0 min to t = 7 min. Methanol was increased from 0 to 20% from t = 7 min to t = 16 min. 4-Nitrobenzenesulfonic acid (**NBS**) was used as an internal standard. The reactant **UpU** and products 2′: 3′-cUMP, 3′-UMP, 2′-UMP, and uridine were identified by comparison of retention time with those of authentic materials. The retention times for the reactant, products, and internal standard under these conditions are as follows: 2′:3′-cUMP, 5.4 min; 3′-UMP 6.9 min; 2′-UMP 7.9 min; uridine 13.3 min; **UpU** 17.9 min; **NBS** 16.0 min. In a typical experiment, solutions contained Eu_2(**1**) (0.5−2.0 mM), **NBS** (0.20 mM), Hepes (20 mM), and $NaNO_3$ (0.10 M). The pH of the solution was adjusted to 7.6, and the solution was incubated at 25 °C. Experiments were initiated by addition of **UpU** (0.040 mM), and the sample was kept at 25 °C throughout the experiment. The percent conversion of reactant (f) was calculated as the ratio of the substrate concentrations at time = t and time = 0 (eq 2).

$$\ln(f) = \ln\left(\frac{[S]_t}{[S]_{t=0}}\right) = -k_{obsd}t \quad (2)$$

For the monomeric catalyst, the concentration of catalyst ranged from 1.0 to 4.0 mM and the **UpU** concentration was 0.080 mM. At t = 0 and at appropriate time intervals, 35 μL aliquots were withdrawn, mixed with the same volume of quenching solution, and stored in a freezer for HPLC analysis. The percent conversion of product (f) was calculated as the ratio of the uridine concentration at time = t and the concentration of reactant at time = 0 (eq 3).

$$\frac{[\text{uridine}]}{[\mathbf{UpU}]_0} = k_{obsd}t \quad (3)$$

Luminescence Spectroscopy. Eu(III) excitation spectra and excited-state lifetimes were obtained using a Spectra-Physics Quanta Ray PRO-270-10 Q-switched Nd:YAG pump laser (10 Hz, 60−70 mJ/pulse) and a MOPO SL for all luminescence measurements. Briefly, the $^7F_0 \rightarrow {}^5D_0$ transition of the Eu(III) ion was scanned between 578 and 582 nm while the $^5D_0 \rightarrow {}^7F_2$ emission band was monitored by using a band pass filter (628 ± 27 nm). Excitation spectra were fit by using the program Peak Fit 4.12 (Jandel). Time-resolved luminescence measurements were collected by using a digital Tektronix TDS 3034B oscilloscope. Data were fit to a single exponential decay by using Sigmaplot version 9.01 (Systat). Solutions contained 0.10 M $NaNO_3$ and 20 mM buffer with Eu(III) complex concentrations varying from 0.10 to 1.0 mM.

The binding constants for Eu_2(**1**) and Eu(**4**) to **MP**, **DEP**, **UpU**, or **NBS** were determined by following the decrease in luminescence intensity, and the data were fit to eq 4.[27] Here C is the Eu(III) macrocyclic complex, CA is Eu(III) macrocyclic anion complex,

(32) Yang, M.-Y.; Morrow, J. R.; Richard, J. P. *Bioorg. Chem.* **2007**, *35*, 366–374.

Scheme 1

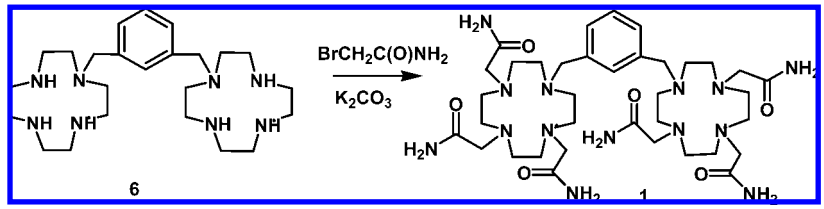

Scheme 2[a]

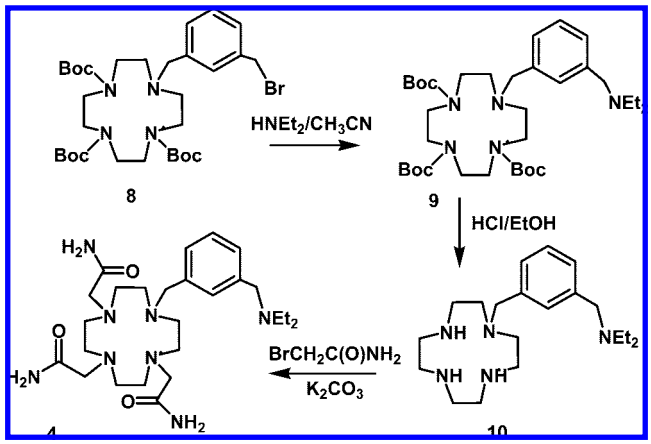

[a] Boc = *t*-butoxycarbonyl.

A is the anionic ligand concentration, X is mole fraction, and I is luminescence intensity at a chosen wavelength. The solutions contained 0.10 mM Eu(**4**) or 0.033−0.50 mM Eu_2(**1**) complex, 20 mM buffer, 0.10 M $NaNO_3$, and 0−2.0 mM **MP**, 0−20 mM **DEP**, 0−4.0 mM **UpU**, or 3.0 mM **NBS**.

$$F = [\mathrm{C}]_{\mathrm{tot}} + [\mathrm{A}]_{\mathrm{tot}} + K_{\mathrm{d}}$$

$$[\mathrm{CA}] = \frac{F - \sqrt{F^2 - 4[\mathrm{C}]_{\mathrm{tot}}[\mathrm{A}]_{\mathrm{tot}}}}{2}$$

$$X_{\mathrm{CA}} = \frac{[\mathrm{CA}]}{[\mathrm{C}]_{\mathrm{tot}}}$$

$$X_{\mathrm{C}} = 1 - X_{\mathrm{CA}}$$

$$I_{\mathrm{obsd}} = X_{\mathrm{C}} I_{\mathrm{C}} + X_{\mathrm{CA}} I_{\mathrm{CA}} \qquad (4)$$

Results

Synthesis of Ligands and Complexes. Dinuclear ligands **1** and **2** were prepared by alkylation of compounds containing two cyclen macrocycles connected through xylyl linkers (cyclen = 1,4,7,10-tetraazacyclododecane, Scheme 1, compound **6**).[30] This method proved to be superior to alternative synthetic routes[33,34] that link macrocycles already containing three pendent amide groups. Two new mononuclear ligands were also prepared. Macrocycle **3** was prepared by methylation of ligand **5** with methyl iodide. Macrocycle **4** was prepared from **8**[31] by treatment with diethylamine (Scheme 2). Subsequently, the amine groups of **9** were deprotected and pendent amide groups were added to give macrocycle **4**. All four macrocyclic ligands were treated with $Eu(CF_3SO_3)_3$ in methanol to give the Eu(III) complexes in good yield.

Solution Chemistry of Eu(III) Complexes. Direct excitation Eu(III) luminescence spectroscopy[22,35−37] was used to characterize the solution speciation of the Eu(III) complexes over the pH range of 7−9 and to monitor binding of phosphate esters. In these studies, the $^7F_0 \rightarrow {}^5D_0$ transition was excited and the intense luminescence emission band ($^5D_0 \rightarrow {}^7F_2$) was monitored. The $^7F_0 \rightarrow {}^5D_0$ transition occurs between two electronic states that are nondegenerate and thus not split by ligand fields, leading to a single excitation peak for each Eu(III) complex species. The Eu(III) complexes were further characterized by time-resolved luminescence experiments. Luminescence lifetimes of Eu(III) complexes are strongly affected by nonradiative processes such as vibronic coupling to ligand groups, especially the OH groups of water or alcohol ligands. The number of bound waters (q) are estimated from measurements of the luminescence lifetimes of the complex in H_2O and D_2O.[35,38] This data is used in eq 5 to calculate q where k_{H2O} and k_{D2O} are the rate constants for luminescence decay in H_2O and D_2O, respectively.[35] Additional contributions to quenching arise from ligand NH groups and from outer-sphere water molecules. These terms are grouped into k_{XH}.

$$q = A[k_{\mathrm{H2O}} - k_{\mathrm{D2O}} - k_{\mathrm{XH}}] \qquad (5)$$

$$k_{\mathrm{XH}} = \alpha + \delta n_{\mathrm{O{=}CNH}} \qquad (6)$$

Quenching constants vary slightly for different classes of Eu(III) complexes, so we chose values ($\alpha = 0.25$ ms^{-1} for outer-sphere contribution, $\delta = 0.075$ ms^{-1} for amide NH, $A = 1.2$ ms) that were reported for Eu(III) complexes with similar structures.[35,38,39] In particular, the quenching value for N−H in the macrocyclic ring (i.e., Eu(**5**)) has not been extensively studied, and we use a value determined recently for a similar class of complexes.[16] Outer-sphere quenching contributions (α) vary from 0.15 to 0.31 ms^{-1} depending on the overall charge on the Eu(III) complexes and the hydrophilic character of the pendent groups.[39] Outer-sphere quenching contributions from weakly coordinating anions present at high concentrations may have a small contribution as well.[40−42]

Luminescence spectroscopy studies of the four Eu(III) complexes of **1**−**4** show evidence of the stereoisomerism that

(33) Harte, A. J.; Jensen, P.; Plush, S. E.; Kruger, P. E.; Gunnlaugsson, T. *Inorg. Chem.* **2006**, *45*, 9465–9474.
(34) Pope, S. J. A.; Kenwright, A. M.; Boote, V. A.; Faulkner, S. *Dalton Trans.* **2003**, 3780–3784.
(35) Supkowski, R. M.; Horrocks, W. D. *Inorg. Chim. Acta* **2002**, *340*, 44–48.
(36) Latva, M.; Takalo, H.; Mukkala, V.-M.; Kankare, J. *Inorg. Chim. Acta* **1998**, *267*, 63–72.
(37) Choppin, G. R.; Wang, Z. M. *Inorg. Chem.* **1997**, *36*, 249–252.
(38) Parker, D.; Dickins, R. S.; Puschmann, H.; Crossland, C.; Howard, J. A. K. *Chem. Rev.* **2002**, *102*, 1977–2010.
(39) Beeby, A.; Clarkson, I. M.; Dickins, R. S.; Faulkner, S.; Parker, D.; Royle, L.; de Sousa, A. S.; Williams, J. A. G.; Woods, M. *J. Chem. Soc., Perkin Trans. 2* **1999**, 493–503.
(40) Billard, I.; Rustenholtz, A.; Semon, L.; Lutzenkirchen, K. *Chem. Phys.* **2001**, *270*, 345–354.
(41) Nehlig, A.; Elhabiri, M.; Billard, I.; Albrecht-Gary, A.-M.; Lutzenkirchen, K. *Radiochim. Acta* **2003**, *91*, 37–43.
(42) Rustenholtz, A.; Billard, I.; Duplatre, G.; Lutzenkirchen, K.; Semon, L. *Radiochim. Acta* **2001**, *89*, 83–89.

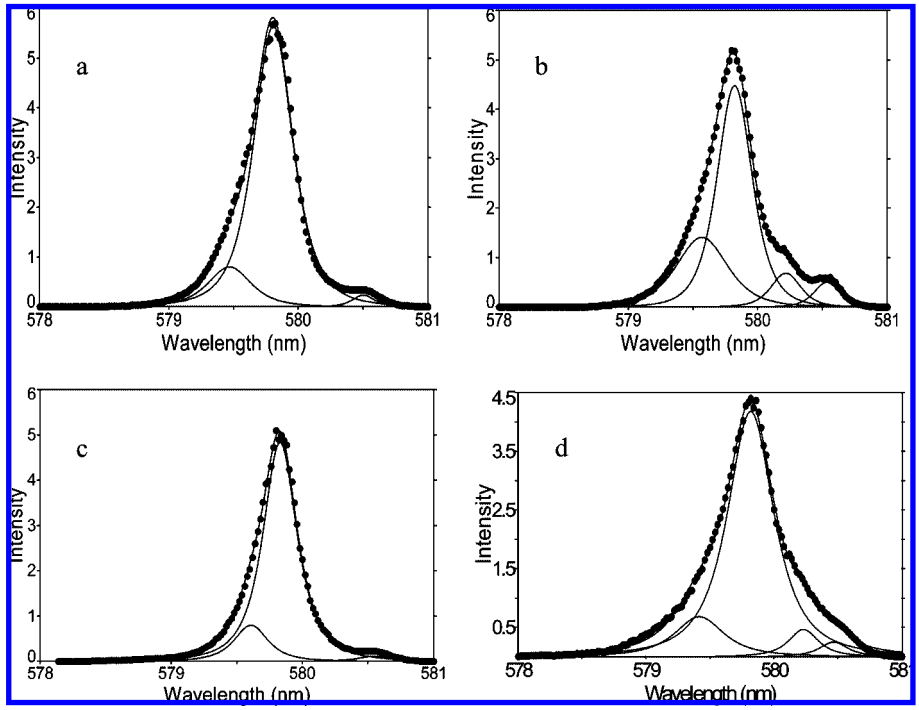

Figure 1. $^7F_0 \rightarrow {}^5D_0$ excitation spectra ($^5D_0 \rightarrow {}^7F_2$ emission) of solutions of (a) Eu_2(**1**), (b) Eu_2(**2**), (c) Eu(**3**), and (d) Eu(**4**), 1.0 mM complex at pH 7.0, buffer = 20 mM, I = 0.10 M $NaNO_3$.

is characteristic of cyclen-based macrocycles. The stereoisomerism displayed by monomeric Ln(III) complexes of cyclen derivatives with pendent groups involves two elements of chirality. One arises from the pendent group orientation (clockwise or counterclockwise) and the other from the two conformations of the tetraazamacrocyclic ring.[38,43] This gives rise to two different diastereomers including one with twisted square antiprismatic (TSAP) geometry and the other with square antiprismatic (SAP) geometry.[44,45] In solution, it is common to observe both isomers although generally one predominates in solution. Previous work in our laboratory showed that the two diastereomers of the monomeric diaqua complex Eu(**5**)$(H_2O)_2$ each gave rise to a separate $^7F_0 \rightarrow {}^5D_0$ excitation peak[14,16] and that one of the diastereomeric forms predominated in solution.[44] The excitation luminescence spectra of Eu_2(**1**), Eu_2(**2**), Eu(**3**), and Eu(**4**) contain peaks that we assign to the two diastereomeric forms of their aqua complexes in solution, analogous to Eu(**5**)$(H_2O)_2$. These Eu(III) complexes of **1**−**4** also contain one to two red-shifted peaks in their excitation spectrum that we attribute to carbonate complexes as discussed below. The two peaks assigned as the SAP and TSAP diastereomers are at similar wavelengths for all complexes: Eu_2(**1**), 579.82, 579.50 nm; Eu_2(**2**) 579.84, 579.55 nm; Eu(**3**), 579.83, 579.62 nm; Eu(**4**), 579.82, 579.54 nm, as shown in Figure 1. The pH independence of these peaks for Eu(III) complexes of **1** and **3** (Supporting Information Figures S1 and S3) and the similarity of peak position to analogous complexes[16] are consistent with their assignment as the two diastereomers. Further support is given by the invariability of the luminescence lifetimes for the major species of the Eu(III) complexes of **1**−**3** over the pH range of 7.0−9.0, consistent with a single species in solution under these conditions (data not shown). Luminescence lifetime data for Eu(III) complexes of **1**−**4** taken at the wavelength maximum of the major peak shows that the major species for all complexes has approximately two bound waters for each Eu(III) center (Table 1). This is consistent with septadentate macrocyclic ligands and nine-coordinate Eu(III) complexes.

Table 1. Luminescence Lifetime Data and Number of Bound Waters (q) for Eu(III) Complexes

complex[a]	λ (nm)	τ_{H2O} (ms)	k_{H2O} (ms^{-1})	τ_{D2O} (ms)	k_{D2O} (ms^{-1})	q
Eu_2(**1**)	579.82	0.31	3.2	1.7	0.60	1.8
Eu_2(**2**)	579.84	0.30	3.3	1.7	0.60	1.9
Eu(**3**)	579.83	0.32	3.1	1.6	0.61	2.1
Eu(**4**)	579.82	0.33	3.0	1.5	0.66	1.9
Eu(**5**)[b]	580.08	0.26	3.9	1.6	0.64	2.0

[a] 0.50 mM complex, 20 mM Hepes, pH 7.0, I = 0.10 M ($NaNO_3$). [b] Ref 16.

The small red-shifted peak at 580.55 nm for Eu_2(**1**) and at 580.62 nm for Eu(**3**) grows in over a period of several days and is more intense at high pH (Supporting Information Figures S1−S3). Similarly, Eu_2(**2**) and Eu(**4**) have two minor red-shifted peaks at 580.22 and 580.55 nm and 580.12 and 580.48 nm, respectively. We assign these peaks to carbonate complexes based on the increase in intensity of these peaks upon addition of sodium carbonate to a solution of Eu_2(**1**), Eu(**3**), Eu(**4**), or Eu_2(**2**) at pH 7.0 (Supporting Information Figures S4−S7). Excitation at the wavelength maximum of these peaks gives luminescence lifetimes that correspond to an absence of bound water ligands (Supporting Information Table S1). Thus, the two peaks likely arise from two different diastereomeric complexes with a bidentate carbonate ligand, similar to observations made by Bruce et al. with monomeric Eu(III) complexes.[46] All attempts to eliminate contamination with carbonate in solutions failed to further decrease the intensity of these peaks, presumably because carbonate binds avidly to these complexes. The

(43) Aime, S.; Botta, M.; Ermondi, G. *Inorg. Chem.* **1992**, *31*, 4291–4299.
(44) Aime, S.; Barge, A.; Bruce, J. I.; Botta, M.; Howard, J. A. K.; Moloney, J. M.; Parker, D.; de Sousa, A. S.; Woods, M. *J. Am. Chem. Soc.* **1999**, *121*, 5762–5771.
(45) Aime, S.; Barge, A.; Botta, M.; De Sousa, A. S.; Parker, D. *Angew. Chem., Int. Ed.* **1998**, *37*, 2673–2675.

Chart 1

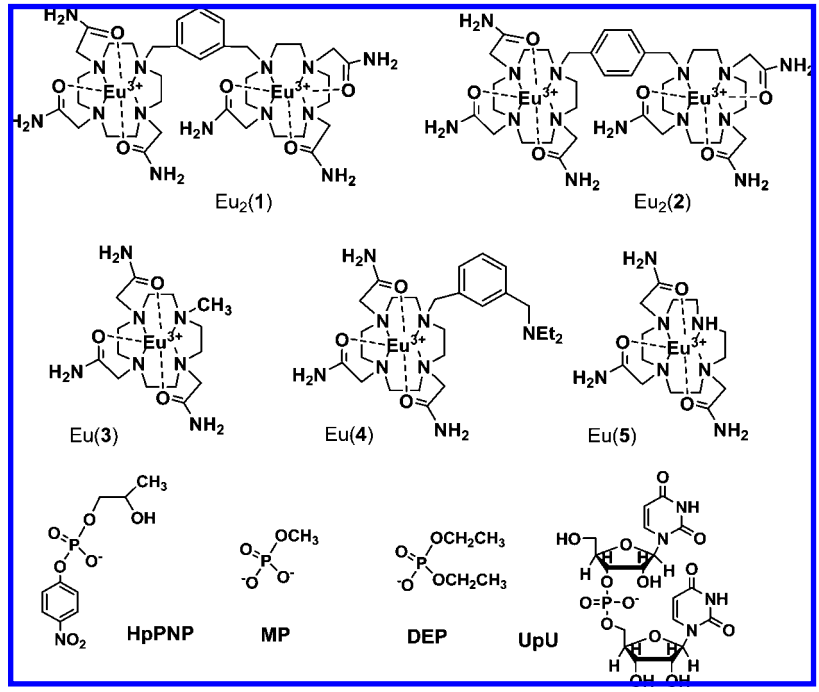

formation of carbonate complexes and precipitates at high pH (>9.5) precluded the analysis of water ligand ionization constants.

Binding constants of phosphate esters to the Eu(III) complexes were measured to give insight into the role of these catalysts in RNA cleavage. Binding of a phosphate diester, **DEP** (Chart 1), and a phosphate monoester, **MP**, to dinuclear and mononuclear Eu(III) complexes was studied by luminescence spectroscopy and by kinetic inhibition studies. Luminescence binding titrations were carried out on Eu_2(**1**), because there is less interference from carbonate adducts and on Eu(**4**) and Eu(**5**) as examples of mononuclear complexes.

Europium excitation spectra of Eu(**4**) (Supporting Information Figure S8) titrated with **MP** show a decrease in the intensity of the original major excitation peak as **MP** binds to the Eu(III) complex. This decrease in luminescence intensity is used to determine a dissociation constant by fitting the data to eq 4 for formation of a 1:1 complex between Eu(**4**) and **MP**. Dissociation constants are given in Table 2.

The excitation spectra of Eu_2(**1**) titrated with **MP** is shown in Figure 2. The peak-fitted excitation spectra of Eu_2(**1**) with bound **MP** (Supporting Information Figure S10) shows that there are two distinct Eu(III) centers. The small frequency separation between the peaks suggests that these species are isomers of each other, possibly arising from the different diastereomeric forms imparted by the macrocyclic ligand. Eu_2(**1**) binds to a single equivalent of **MP** (Supporting Information Figure S11), and the data was accordingly fit to eq 4 for 1:1 binding[27] with the binding constant given in Table 2 (Figure 3).

To determine whether a single or both Eu(III) centers in Eu_2(**1**) interact with **MP**, and whether **MP** replaces a water ligand upon binding to Eu(III) complexes, luminescence lifetimes as a function of **MP** concentration were measured for Eu_2(**1**), and values of bound water molecules (q) were calculated. These data show that one bound water per Eu(III) ion in Eu_2(**1**) is replaced by the phosphate ester ($q \sim 1$) (Supporting Information Table S1). Luminescence lifetime data at all points in the titration fit to a single exponential, consistent with rapid

Table 2. Dissociation Constants at 25 °C, $I = 0.10$ M ($NaNO_3$), pH 7.6, 20 mM Hepes for Eu(III) and Zn(II) Complexes with Phosphate Esters[a]

complex	K(MP, mM)	ΔG_{MP} (kcal/mol)	K(DEP, mM)	ΔG_{DEP} (kcal/mol)
Eu_2(**1**)	0.060 (0.025)[b]	5.8 (6.3)[b]	0.43	4.6
Eu(**5**)	0.28	4.9	7.5	2.9
Eu(**4**)	0.018[b]	6.5[b]		
Eu(**3**)	0.18	5.1	2.7	3.5
Zn(**12**)[c]	14	2.5	94	1.4
Zn_2(**13**)[c]	0.010	6.9	16	2.5

[a] Obtained from kinetic inhibition experiments except where noted. [b] From luminescence titration, average of three measurements. [c] From ref 20 and 32.

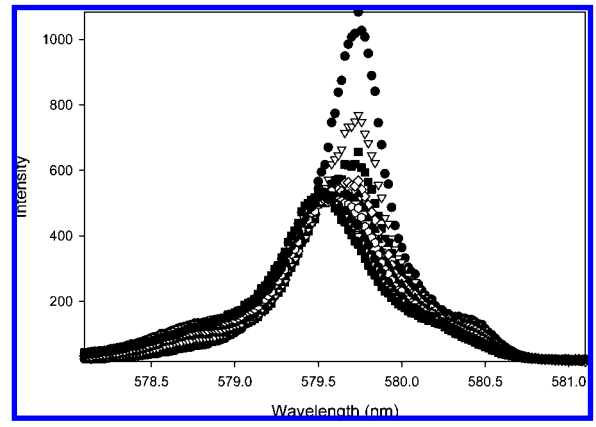

Figure 2. $^7F_0 \rightarrow {}^5D_0$ excitation spectra ($^5D_0 \rightarrow {}^7F_2$ emission) of solutions of 3.30 μM Eu_2(**1**) at pH 7.6 titrated with 25−380 μM **MP** showing a decrease in the intensity of peaks at 579.82 and 580.55 nm.

(46) Bruce, J. I.; Dickins, R. S.; Govenlock, L. J.; Gunnlaugsson, T.; Lopinski, S.; Lowe, M. P.; Parker, D.; Peacock, R. D.; Perry, J. J. B.; Aime, S.; Botta, M. *J. Am. Chem. Soc.* **2000**, *122*, 9674–9684.

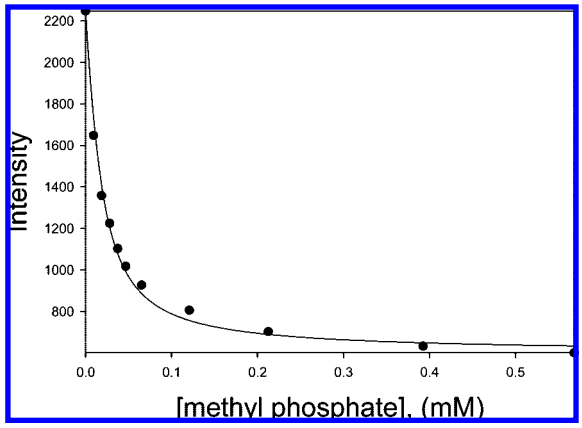

Figure 3. Plot of observed luminescent intensity (579.82 nm) of Eu_2(**1**) (3.30 μM) as a function of total added **MP** concentration at 25 °C, I = 0.10 M $NaNO_3$, pH 7.6, 20 mM Hepes. The solid curve represents the best fit to eq 4 with K_d = 23 μM.

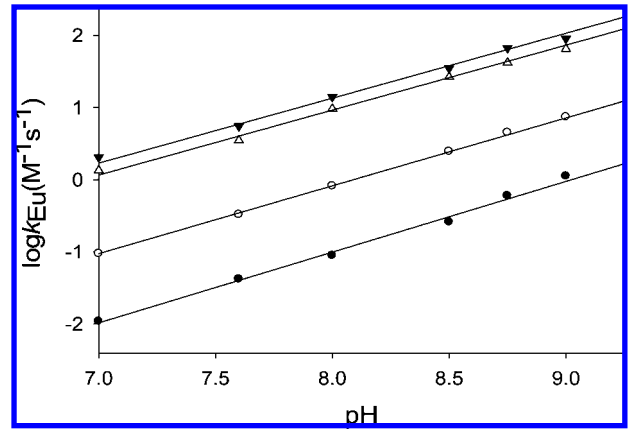

Figure 4. pH rate profile of second-order rate constants for cleavage of **HpPNP** by Eu(**5**) (●), Eu(**3**) (○), Eu_2(**1**) (▼), and Eu_2(**2**) (△). The solid lines through the values for second-order rate constants (k_{Eu}) show the theoretical fits of these data to the logarithmic form of eq 8.

phosphate ester exchange on the luminescence time scale. For comparison, luminescence lifetime data on Eu(**5**) (Supporting Information Table S2) also showed that a single water molecule was displaced upon formation of Eu(**5**)(**MP**), similar to phosphate binding to analogous Eu(III) mononuclear macrocyclic complexes.[47,48] Binding of **MP** to Eu_2(**1**) was studied over a range of concentrations of the complex including 3.30, 16.7, and 50.0 μM. The similarity in binding constant values (K_d = 23, 29, 23 μM, respectively) shows that binding is independent of catalyst concentration and thus does not involve the formation of a higher aggregate. Taken together, these data show that the **MP** bridges the two Eu(III) centers in Eu_2(**1**).

Binding of **DEP** to Eu_2(**1**) was studied by excitation luminescence spectroscopy (Supporting Information Figures S12 and S13). The peak-fitted excitation spectrum (Supporting Information Figure S14) shows two new peaks similar to that observed upon **MP** binding to Eu_2(**1**) and consistent with two isomeric forms of the complex. Luminescence lifetimes taken as a function of **DEP** concentration show that the number of bound water molecules (q in Supporting Information Table S1) per Eu(III) ion in the complex is reduced to a single bound water upon binding of the phosphate diester, signifying that both Eu(III) centers are bound to **DEP**. We favor binding of a single **DEP** to the dinuclear complexes based on the similarity of the excitation spectrum of the Eu_2(**1**)(**DEP**) complex (Supporting Information Figure S14) to that of the Eu_2(**1**)(**MP**) complex (Supporting Information Figure S10) that shows two closely spaced Eu(III) excitation peaks. However, a 2:1 complex (Eu_2(**1**)(**DEP**)$_2$) cannot be ruled out from our data. Titration of the mononuclear complex, Eu(**5**), with **DEP** also leads to displacement of a single water ligand (Supporting Information Table S2).

Cleavage of HpPNP. Eu(III) complexes of **1**−**5** catalyze the cleavage of **HpPNP** as followed by monitoring the increase in absorbance at 400 nm due to formation of 4-nitrophenolate anion. Cleavage occurs by an intermolecular transesterification process as shown by identification of the cyclic phosphate ester as the sole phosphorus-containing product by using ^{31}P NMR spectroscopy.

Scheme 3

$$\mathbf{HpPNP} + \mathbf{Eu(L)} \xrightarrow{k_T[OH^-]} \mathbf{products}$$

Pseudo-first-order rate constants (k_{obsd}, s^{-1}) for the cleavage of **HpPNP** were determined for a range of catalyst concentrations. The second-order rate constants (k_{Eu}, M^{-1} s^{-1}) at 25 °C, I = 0.10 M ($NaNO_3$) for the cleavage of **HpPNP** catalyzed by the Eu(III) complexes were determined as the slopes of the plots of k_{obsd} against catalyst by fitting to eq 7 (as shown in Supporting Information Figure S15), and the values are listed in Supporting Information Table S3. Second-order rate constants were determined over a pH range that was limited by the solubility properties of each catalyst. Only one pH value was studied for Eu(**4**) because of the low solubility of the complex at higher pH values. For the other four complexes, plots of the log of the second-order rate constants as a function of pH are shown in Figure 4 along with the data for complex Eu(**5**), as determined previously.[16] Eu(III) macrocyclic complexes (**1**−**3** and **5**) showed a linear dependence of second-order rate constant on pH, and the data was fit to eq 8 derived for Scheme 3.

$$k_{obs} = k_{Eu}[\mathrm{Eu}(\mathbf{L})] \quad (7)$$

$$k_{Eu} = k_T[OH^-] \quad (8)$$

Cleavage of UpU. The progress of the cleavage reaction of **UpU** catalyzed by Eu_2(**1**) at pH 7.6 and 25 °C was monitored by HPLC. Each substrate peak area was normalized to that of the internal standard. The observed first-order rate constant (k_{obsd}, s^{-1}) was determined as the negative slope of logarithmic fraction (ln(f)) against time (eq 2). Supporting Information Figure S16 shows representative plots of logarithmic fractional conversion of **UpU** to products over time. Supporting Information Figure S17 shows a plot of first-order rate constant as a function of Eu_2(**1**) concentration (1−4 mM), whose slope is the second-order rate constant (0.021 M^{-1} s^{-1}). A complicating feature of these reactions is that the HPLC internal standard, **NBS**, binds to Eu_2(**1**) nearly as strongly as does **UpU** (K_d = 1.4 mM, **NBS**; K_d = 0.72 mM, **UpU**) (Supporting Information Figures S18−21) and is present in excess over **UpU**, serving to weaken the effective binding constant of the catalyst to **UpU** substrate. Under these conditions with 2.0 mM catalyst, we calculate that only 20% is complexed to **UpU**, in contrast to the 80%

(47) Atkinson, P.; Bretonnière, Y.; Parker, D.; Muller, G. *Helv. Chim. Acta* **2005**, *88*, 391–405.
(48) Atkinson, P.; Bretonniere, Y.; Parker, D.; Muller, G. *Helv. Chim. Acta* **2005**, *88*, 391–405.

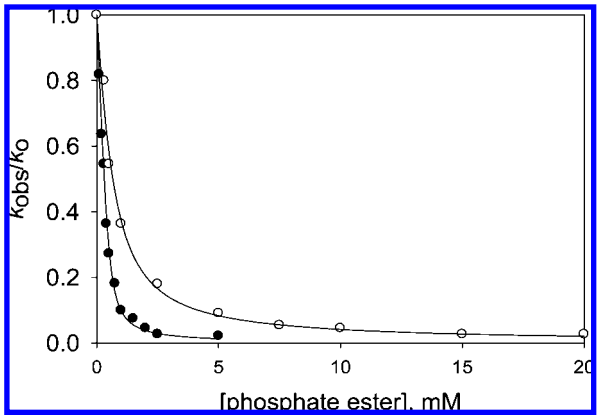

Figure 5. Diethyl phosphate (**DEP**) and monomethyl phosphate (**MP**) inhibition of the Eu_2(**1**) complex (MP (●), DEP (○)) catalyzed cleavage of **HpPNP** at 25 °C, I = 0.10 M ($NaNO_3$), pH 7.6, 20 mM Hepes buffer. Data is fit to eq 1 with K_i = 0.060 mM for **MP** and 0.43 mM for **DEP**.

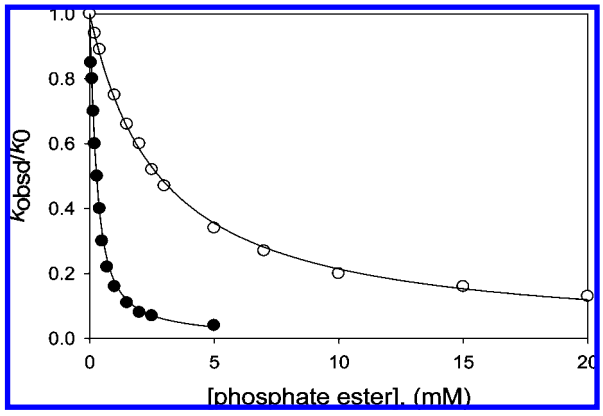

Figure 6. Diethyl phosphate (**DEP**, ○) and monomethyl phosphate (**MP**, ●) inhibition of the Eu(**3**) (0.2 mM) catalyzed cleavage of **HpPNP** at 25 °C, I = 0.10 M ($NaNO_3$), pH 7.6, 20 mM Hepes. Data is fit to eq 1 with K_i = 2.7 mM for **DEP** and 0.18 mM for **MP**.

complexed in the absence of the sulfonate internal standard. This leads to the observed linear dependence of the reaction rate constant on catalyst concentration.

The progress of the cleavage reaction of **UpU** catalyzed by Eu(**5**) at pH 7.6 and 25 °C was monitored by HPLC for the appearance of uridine. The observed first-order rate constant (k_{obsd}, s^{-1}) was determined as the slope of fraction (f) against time over the first 2−6% of reaction (eq 3; Supporting Information Figure S22). A plot of first-order rate constant as a function of Eu(**5**) concentrations, whose slope is the second-order rate constant (4.4×10^{-4} M^{-1} s^{-1}), is shown in Supporting Information Figure S23.

Binding constants of Eu_2(**1**) and Eu(**3**) to **MP** and **DEP** were obtained by competitive inhibition of **HpPNP** cleavage. Normalized plots of the first-order rate constants at varying concentrations of phosphate ester as an inhibitor are shown in Figures 5 and 6. Data for **MP** binding was fit to eq 1, derived from Scheme 4 for 1:1 binding of **MP** to the Eu(III) complexes. Equation 1 is used to accommodate the tight binding of the complexes to the phosphate esters. Inhibition constants are given in Table 2.

Discussion

Reaction Mechanism. The kinetic data for **HpPNP** cleavage by the complexes examined here, Eu_2(**1**), Eu_2(**2**), Eu(**3**), Eu(**5**),

Scheme 4

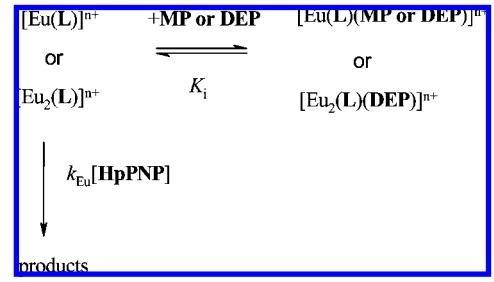

Chart 2

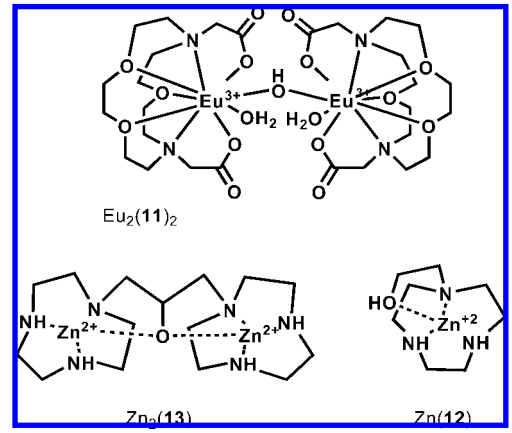

and for a dimeric complex studied previously (Eu_2(**11**)$_2$, Chart 2)[28] show strikingly similar characteristics. For all complexes, the log of the second-order rate constants plotted as a function of pH shows a simple linear dependence on pH for the pH range examined, typically 7−9. This data is consistent with the relatively simple solution speciation behavior of these Eu(III) catalysts over a broad pH range including no water ligand ionization under these conditions. This contrasts to the pH−rate profile observed for metal ion complexes that have water ligand ionizations within the studied pH range. For example, second-order rate constants for the cleavage of **HpPNP** catalyzed by Zn(II) complexes (Zn(**12**) and Zn_2(**13**) in Chart 2) are linear as a function of pH at low pH but demonstrate a downward break at the pK_a value of the Zn−H_2O where pH > pK_a.[18,20,32,49,50]

The pH rate profile of **HpPNP** cleavage for these Eu(III) and Zn(II) complexes is consistent with a proton being lost from the substrate or catalyst on going to the transition state. Two mechanistic pathways by which this loss of proton may proceed[19,21,32] include (1) loss of the proton from the catalyst to form a M(**L**)(OH) complex that interacts with the substrate as a general base catalyst in the rate-limiting step or (2) loss of the proton from the substrate 2′-hydroxyl in a pre-equilibrium step followed by interaction of M(**L**)(OH_2) with the deprotonated substrate in the rate-limiting step (Scheme 5, left and right side, respectively). Our work with deuterium solvent isotope studies of the cleavage of an RNA analogue shows that there no Brønsted general base catalysis[19] in the presence of metal ion

(49) Yang, M.-Y.; Richard, J. P.; Morrow, J. R. *Chem. Commun.* **2003**, 2832–2833.
(50) Mathews, R. A.; Rossiter, C. S.; Morrow, J. R.; Richard, J. P. *Dalton Trans.* **2007**, 3804–3811.
(51) Morrow, J. R.; Amyes, T. L.; Richard, J. P. *Acc. Chem. Res.* **2008**, *41*, 539–548.
(52) Rossiter, C. S.; Mathews, R. A.; Morrow, J. R. *J. Inorg. Biochem.* **2007**, *101*, 925–934.

Scheme 5

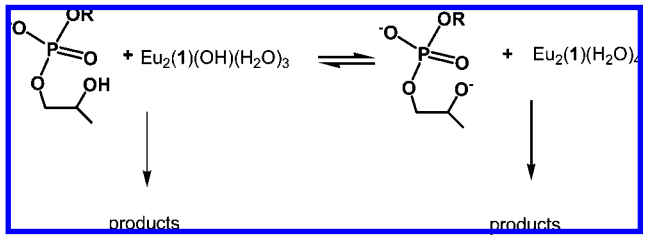

Table 3. Rate Constants for **HpPNP** Cleavage by Eu(III) and Zn(II) Complexes at 25 °C, 20 mM buffer, $I = 0.10$ M ($NaNO_3$)

complex	k_2 (M^{-1} s^{-1})[a]	k_T (M^{-2} s^{-1})[b]	k_T/k_{OH} (M^{-1})[c]	$\Delta G_s^{\ddagger}$ (kcal/mol)[d]
Eu_2(**1**)	5.5	8.7×10^6	8.7×10^7	−10.8
Eu_2(**2**)	3.5	6.4×10^6	6.4×10^7	−10.7
Eu(**3**)	0.33	7.0×10^5	7.0×10^6	−9.4
Eu(**4**)[e]	0.32			
Eu(**5**)[f]	0.042	1.2×10^5	1.2×10^6	−8.3
Zn(**12**)[g]	0.0013	3.8×10^3	3.8×10^4	−6.2
Zn_2(**13**)[g]	0.25	1.1×10^6	3.8×10^7	−9.6
Eu_2(**11**)$_2$[h]		4.0×10^4	4.0×10^5	−7.6

[a] Second-order rate constant at pH 7.6. [b] Apparent third-order rate constant for the metal complex catalyzed reaction in the pH range where there is a first-order dependence on hydroxide. [c] Rate acceleration in the pH range where both metal complex catalyzed and background reaction are first order in hydroxide for $k_{OH} = 0.099$ M^{-1} s^{-1}. [d] Stabilization of the transition state from eq 9. [e] At pH 7.0. [f] From ref 16. [g] From ref 20. [h] From ref 28.

catalysts, in support of the pathway shown on the right of Scheme 5. In addition, experiments show that the M(**L**)(OH_2) species but not the M(**L**)(OH) species binds strongly to dianionic phosphate esters such as **MP**. The interaction of the dianionic **MP** with a metal complex represents the electrostatic component of metal ion stabilization of the dianionic phosphorane transition state.[21,32]

Metal Ion Cooperativity. Two metal ion cooperativity in RNA cleavage is desirable for the formation of highly effective catalysts. Yet, the extent of metal ion cooperativity is difficult to identify because dinuclear catalysts must be compared to mononuclear catalysts[20] that have subtle differences in donor groups. To make rigorous comparisons, we have advocated the use of apparent third-order rate constants for cleavage, calculated as the slope of a plot of second-order rate constants as a function of [OH^-] at pH values less than the pK_a of the metal water ligand.[18,28,50] This facilitates comparisons between catalysts with different water ligand ionization constants. Comparison of third-order rate constants for Eu(III) complexes of **1**−**3** and **5** (k_T in Table 3) shows that the most active Eu(III) dinuclear catalyst is 70-fold better than the mononuclear catalyst Eu(**5**), but only 12-fold better than the methylated version, Eu(**3**). Eu(**4**), which has an aromatic pendent group most closely related to that in the dinuclear complexes, is the best choice of a mononuclear catalyst for comparison. We could not obtain a pH dependence for this complex, but its second-order rate constant at pH 7.0 is 3-fold higher than that of Eu(**3**) and only 7-fold less than that of the best dinuclear catalyst under these conditions (Supporting Information Table S3). This shows that the ancillary pendent group is a dominant factor in enhancing the reactivity of the Eu(III) center and that the analysis of cooperativity between two metal ion centers in a dinuclear complex is dependent on the choice of appropriate mononuclear catalyst.

$$\Delta G_s^{\ddagger} = \Delta G_E^{\ddagger} - \Delta G_N^{\ddagger} = RT \ln\left[\frac{k_{Eu}K_a/K_w}{k_{OH}}\right] \qquad (9)$$

Scheme 6

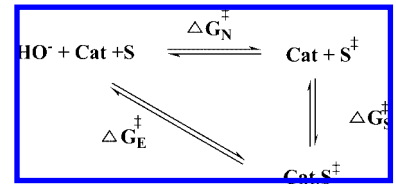

Another type of comparison is provided by the division of the apparent third-order rate constant for cleavage of **HpPNP** by the second-order rate constant for hydroxide promoted cleavage of **HpPNP** (k_T/k_{OH} in Table 3). This gives a rate constant that expresses the magnitude of the binding interaction of the catalyst with the transition state.[16,28,50,51] The free energies derived from this interaction (Scheme 6) represent the transition state stabilization of the reaction by the catalyst ($\Delta G_s^{\ddagger}$ in eq 9). This analysis shows that the dinuclear catalysts have a transition state binding energy of nearly 11 kcal/mol. Yet, there is only a 1.2 kcal/mol difference between the alkylated mononuclear catalyst Eu(**3**) and the least reactive of the dinuclear catalysts. These small free energy differences suggest that the two Eu(III) centers in the dinuclear catalysts lack strong cooperativity in the cleavage of **HpPNP**. By contrast, there is a 3.4 kcal/mol difference in the Zn(II) mononuclear compared to dinuclear complex in Table 3. The dinuclear Zn(II) complex (Zn_2(**13**)) has a bridging alkoxide group that brings together the two Zn(II) centers to interact with the substrate in a cooperative manner, whereas the dinuclear Eu(III) complexes lack a bridging donor group. To further elucidate the catalytic properties of these complexes, binding to the phosphate esters **DEP**, as a substrate analogue, and **MP**, as a transition state analogue, were analyzed.[21,32,50]

Binding of the Eu(III) complexes to **DEP** is weak. There is little discrimination between the different Eu(III) complexes as there is only a 1.5 kcal/mol free energy difference between the strongest and weakest Eu(III) complex interactions with **DEP**. **DEP** replaces one water ligand on each Eu(III) center in both dinuclear and mononuclear complexes, Eu_2(**1**) and Eu(**5**). This suggests that the phosphate diester substrates studied here (**UpU** and **HpPNP**) bind directly to the Eu(III) centers. **DEP** most likely binds by bridging the two Eu(III) centers in Eu_2(**1**), but this interaction through both Eu(III) centers does not markedly increase the binding constant compared to a mononuclear complex.

Eu(III) complexes of **1**−**4** bind to **MP** more tightly than **DEP** with dissociation constants ranging from 0.018 to 0.28 mM. This 2 kcal increase in binding strength over **DEP** is attributed to the higher anionic charge on **MP** that leads to a stronger interaction with the cationic Eu(III) complexes. Similar to **DEP**, **MP** displaces a water ligand on each Eu(III) center. Binding is strongest for the Eu(III) complexes that contain an aromatic pendent group (Eu(**4**) and Eu_2(**1**)). This shows that the electron-withdrawing aromatic group increases the Lewis acidity of the Eu(III) center to form stronger interactions with anionic ligands. Even an alkyl substituent in Eu(**3**) leads to slightly stronger binding than for the unsubstituted macrocyclic complex, Eu(**5**). These macrocyclic substitutent effects are reminiscent of those

(53) Canary, J. W.; Xu, J.; Castagnetto, J. M.; Rentzeperis, D.; Marky, L. A. *J. Am. Chem. Soc.* **1995**, *117*, 11545–11547.
(54) Cacciapaglia, R.; Casnati, A.; Mandolini, L.; Peracchi, A.; Reinhoudt, D. N.; Salvio, R.; Sartori, A.; Ungaro, R. *J. Am. Chem. Soc.* **2007**, *129*, 12512–12520.

Scheme 7

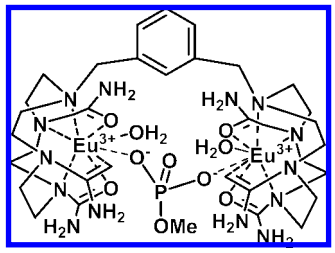

observed for Zn(II) macrocyclic complexes.[32,52,53] For Zn(II) complexes, the decreased interaction of the alkylated macrocyclic amines of the complex with water leads to poor solvation of highly charged cationic complexes and stronger anion binding affinity. Despite these trends, the free energy differences between the mononuclear and dinuclear Eu(III) complexes for binding of **MP** (1.4 kcal) are not very large. By comparison, the free energy for interaction of **MP** to a dinuclear complex (Zn_2(**13**) that likely binds **MP** through a bridging interaction is 4.4 kcal/mol greater than for a related mononuclear Zn(II) catalyst.[32] The difference is that the bridging alkoxide group in Zn_2(**13**) facilitates strong interaction with **MP** through both Zn(II) centers. The dinuclear Eu(III) catalyst Eu_2(**1**) also binds a single **MP** through an intramolecular bridging interaction (Scheme 7), as shown by luminescence spectroscopy experiments. However, the two metal ion centers are not anchored together through a bridging group prior to binding **MP** as they are for the dinuclear Zn(II) catalyst. This lack of preorganization for Eu_2(**1**) may lead to a less favorable interaction with **MP** and, by analogy, a less favorable interaction with the phosphorane that is the likely form of the transition state.

There is a weak correlation between the transition state stabilization energy for these complexes for the cleavage of **HpPNP** (Table 1) and the free energy of binding to the transition state analogue, **MP** (Table 3). Eu_2(**1**) has one of the strongest binding interactions with **MP** and the largest transition state stabilization of Eu(III) complexes **1**−**5**. The poorest catalyst, Eu(**5**), binds to **MP** the most weakly. However, as discussed above, neither the **MP** binding energy difference between mono and dinuclear catalysts Eu(**3**) and Eu_2(**1**) (−5.1 vs −6.3 kcal/mol) nor the difference in free energy for binding the transition state (−9.4 vs −10.8 kcal/mol) are large. This suggests that, despite the interaction of both Eu(III) centers in binding **MP**, **DEP**, and presumably the transition state phosphorane, the second loosely tethered metal ion center is not effective at enhancing binding strength (Scheme 7). Despite the similar trends in strength of **MP** and transition state interactions of the Eu(III) complexes, it is clear that there are other factors important in catalysis that are not expressed in **MP** binding. The 6 kcal/mol free energy of binding of Eu_2(**1**) to **MP** is a fraction of the nearly 11 kcal/mol stabilization of the transition state energy for cleavage of **HpPNP**. Factors not represented include differences in the phosphate ester versus phosphorane geometry and the extent equilibrium solvation of charge.[32]

Although there is little cooperativity between the two metal centers, the dinuclear Eu(III) complexes of **1** and **2** have the largest transition state stabilization energy reported to date by our laboratory for cleavage of **HpPNP** by a simple metal ion catalyst in water at 25 °C.[50] These complexes show a greater than 3 kcal/mol stabilization compared to the dinuclear complex Eu_2(**11**)$_2$. This large stabilization energy is anticipated because macrocycles **1** and **2** bind to Eu(III) to leave open two coordination sites for interaction with substrate and avoid the use of negatively charged carboxylate pendent groups that generally decrease catalytic efficiency. The influence of the ligand donor groups is one of the most important factors in lanthanide catalysis. For example, dinuclear lanthanide catalysts with bridging hydroxyl groups and negatively charge carboxylate groups of amino acids presumably have many more open coordination sites than Eu(III) complexes of **1** or **2** but still are less active than the catalysts here.[1]

Cleavage of UpU. Second-order rate constants for the cleavage of **UpU** at pH 7.0 for Eu_2(**1**) and Eu(**5**) are 0.021 and 4.4 × 10^{-4} M^{-1} s^{-1}, respectively. This shows that cleavage of **UpU** by Eu_2(**1**) at pH 7.6 is 46-fold higher than for Eu(**5**), a little less than the 70-fold difference observed for **HpPNP** cleavage. Comparison to the rate constant for cleavage of **UpU**[18] by hydroxide at pH 7.0 gives transition state stabilization energies (k_T/k_{OH}) of 2.0 × 10^7 (10 kcal/mol) and 3.9 × 10^5 M^{-1} (7.6 kcal/mol), respectively, slightly less than that observed for the cleavage of **HpPNP** by these catalysts. On the basis of the analysis with **HpPNP** and **MP** binding studies, the larger reactivity for the dinuclear complex in the cleavage of **UpU** is attributed to an increase in anion binding affinity of the Eu(III) center by the aryl pendent group and possibly to a small extent of cooperativity between the two Eu(III) centers.

The second-order rate constant for cleavage of **UpU** catalyzed by Eu_2(**1**) is 26-fold larger than Zn_2(**10**) under similar conditions[18] and 2-fold larger than a dinuclear Zn(II) catalyst that has both a bridging alkoxide donor group to promote cooperativity of metal ions and hydrogen bond donors for interactions with the phosphate diester linkage.[52] Comparison with additional multinuclear Cu(II) and Zn(II) catalysts is complicated by the high temperatures generally used in dinucleotide cleavage experiments and by the addition of organic cosolvents to solubilize the complexes.[18,54−56] Recent work on water-soluble dinuclear Cu(II) catalysts shows that first-order rate constants for cleavage of **UpU** at neutral pH at 1.0 mM catalyst and 50 °C are comparable[53] to those observed here for Eu_2(**1**) at the lower temperature of 25 °C.

Apart from the multinuclear metal ion complex catalysts with relatively well-defined solution chemistry, there are examples of metal ion complex catalysts that have poor ligands and form difficult to characterize yet highly active aggregates.[1,5] The most efficient metal ion catalyst for RNA cleavage reported to date is in this category and is a multinuclear species formed at high pH in solutions containing 2 mM $LaCl_3$ and buffer. This complex promotes the cleavage of **ApA** with a half-life of 13 s.[5] Characterization of this labile catalyst is difficult but is thought to contain multinuclear La(III) centers that form at pH > 8 to produce a catalyst that promotes cleavage optimally at pH 9. In comparison, Eu_2(**1**) cleaves **UpU** at near neutral pH with a half-life of 4 h for 2 mM catalyst, a 10^4-fold acceleration over cleavage of **UpU** with no catalyst under these conditions.[18] A challenge to inorganic chemists is to identify the features of

(55) Cacciapaglia, R.; Casnati, A.; Mandolini, L.; Reinhoudt, D. N.; Salvio, R.; Sartori, A.; Ungaro, R. *Inorg. Chim. Acta* **2007**, *360*, 981–986.
(56) Yashiro, M.; Kaneiwa, H.; Onaka, K.; Komiyama, M. *Dalton Trans.* **2004**, 605–610.
(57) Iranzo, O.; Richard, J. P.; Morrow, J. R. *Inorg. Chem.* **2004**, *43*, 1743–1750.

these aggregates that lead to effective catalysis and to transfer these features to catalysts in well-defined complexes.

Conclusion

Lanthanide ion complexes with neutral ligands are highly effective catalysts for the cleavage of phosphate esters and RNA. Anionic phosphate esters bind strongly to these complexes by replacing a water ligand, and this strong inner-sphere interaction is undoubtedly an important one in catalysis. Importantly, at near neutral pH, these lanthanide complexes do not form hydroxide complexes but exist as the aqua complexes that are generally the more reactive form.[16,32,49] This stands in contrast to complexes of Zn(II) and Cu(II) which readily form hydroxide complexes at neutral pH values.[20,50,57] Thus, the selectivity of these lanthanide ion complexes for binding phosphate esters over hydroxide is one important feature of these catalysts. Studies here show that macrocyclic ligands with aromatic pendent groups form Eu(III) complexes that are among the most effective reported to date for cleavage of **HpPNP** and for a dinucleoside, **UpU**, in water at 25 °C. Further improvements may be possible through choice of a linker that has a donor group that bridges the two lanthanide ion centers to preorganize them for interaction with substrate.

Acknowledgment. We gratefully acknowledge the National Science Foundation (CHE0415356) for support of this work and for a major instrumentation award (CHE-0321058) to build the laser system. We thank John Richard for helpful discussions.

Supporting Information Available: Europium(III) excitation luminescence data, binding isotherms for ligands with europium(III) complexes, and kinetic data. This material is available free of charge via the Internet at http://pubs.acs.org.

JA8037799